

Crystal Overgrowth on Gold Nanorods: Tuning the Shape, Facet, Aspect Ratio, and Composition of the Nanorods

Jae Hee Song,^{+[a, b]} Franklin Kim,^{+[a]} Daniel Kim,^[a] and Peidong Yang^{*[a]}

Abstract: Electrochemically prepared Au nanorods were used as seeds for the overgrowth of thin shells of gold, silver, and palladium by using a mild reducing agent, ascorbic acid, in the presence of surfactants at ambient condition. The unique crystal facets of the starting nanorods results in anisotropic crystal overgrowth. The overgrowth rates along different crystallographical

directions can be further regulated by adding foreign ions or by using different metal reduction methods. This overgrowth study provides insights on how different metal ions could be reduced preferentially on different Au

nanorod surfaces, so that the composition, aspect ratio, shape, and facet of the resulting nanostructures can be rationally tuned. These surfactant-stabilized bimetallic Au_{core}M_{shell} (M = Au, Ag, Pd) nanorod colloids might serve as better substrates in surface-enhanced Raman spectroscopy as well as exhibiting enhanced catalytic properties.

Keywords: colloids • crystal growth • gold • nanorods • nanostructures

Introduction

Controlling the shape of nanoparticles is technologically important, since their optical, electronic, magnetic, and catalytic properties often depend critically not only on particle size, but also on particle shape.^[1–3] Hence, a major current research direction is to develop methodology for size- and shape-selective nanocrystal growth. There have been extensive efforts focusing on the development of new synthetic methodologies (e.g., reverse micelle templating, seed-mediated growth, crystal growth regulated by surfactants and co-surfactants, and magic-sized nucleation/growth)^[4–12] for making nanorods with uniform sizes and aspect ratios.

Synthesizing gold nanorods by means of wet chemical routes has been demonstrated in several experimental systems. In all these cases, it is either certain or possible that a templating mechanism is operating. The preparation of poly-

crystalline rodlike gold particles in the nanopores of alumina or polycarbonate membranes by electrochemical reduction is a clear demonstration of the success of a hard template.^[13] Formation of gold nanorods by an electrochemical or photochemical reduction method in a surfactant solution has been demonstrated, and the templating mechanism remains elusive.^[5] Another method to produce long, threadlike gold particles was reported by Esumi.^[14] In their method, gold particles are produced by photochemical reduction in the presence of cationic surfactant micelles. The authors indicated that the templating effect of rodlike micelles is critical to the formation of gold nanowires with diameters of several tens nanometers. More recently, a seeded growth methodology has been introduced to synthesize uniform Au and Ag nanorods.^[7] In this process, Au clusters were used as seeds to initiate the nanorod growth although the exact mechanism for the one-dimensional crystal growth remains unclear.

On the other hand, metal nanoparticles composed of multiple elements are of significant interest from both technological and scientific points of view for improving catalytic activity and properties.^[15–19] The chemical and physical stability, as well as the selectivity of catalytic reactions for these bimetallic nanoparticles would be different from those of monometallic particles. For example, it was found that the Au surface shows a lower enhancement factor in the visible region relative to that of Ag; consequently, the bimetallic Ag–Au particles could serve as better substrates for surface-enhanced Raman spectroscopy (SERS).^[20] For these

[a] Dr. J. H. Song,⁺ F. Kim,⁺ D. Kim, Prof. P. Yang
Department of Chemistry, University of California
Materials Science Division
Lawrence Berkeley National Laboratory
Berkeley, CA 94720 (USA)
Fax: (+1) 510-642-7301
E-mail: p_yang@uclink.berkeley.edu

[b] Dr. J. H. Song⁺
Present address: Department of Chemistry
Sunchon National University
315 Maegok, Suncheon, Jeonnam 540-742 (Korea)

[*] These authors contributed equally to this work.

reasons, many different preparation methods have been reported for synthesis of core-shell nanoparticles. Most of the studies involve chemical, photochemical, or electrochemical reduction of metal ions in the presence of polymers or surfactants, while using spherical nanoparticles as seeds.

Despite many of these studies on bimetallic core-shell nanoparticle preparation, there are only few reports on core-shell metallic nanorods.^[19] In this article, we describe our systematic studies on the general overgrowth behavior on pre-formed Au nanorods. Electrochemically prepared Au nanorods were used as seeds for the overgrowth of thin shells of gold, silver, and palladium by using a mild reducing agent, ascorbic acid, in the presence of surfactants at ambient condition. Since the starting nanorods exhibit unique crystal facets, the overgrowth exhibits interesting features due to competing crystal growth on different side facets. This overgrowth behavior should provide insights on how different metal ions could be reduced preferentially on Au nanorod surfaces so that the composition, aspect ratio, shape, and facet of the resulting nanostructures can be rationally tuned.

Results and Discussion

Au overgrowth on nanorods: Figure 1 shows the UV-visible spectra of Au nanorods with varied HAuCl_4 addition. Before the Au overgrowth, the solution appears light red-

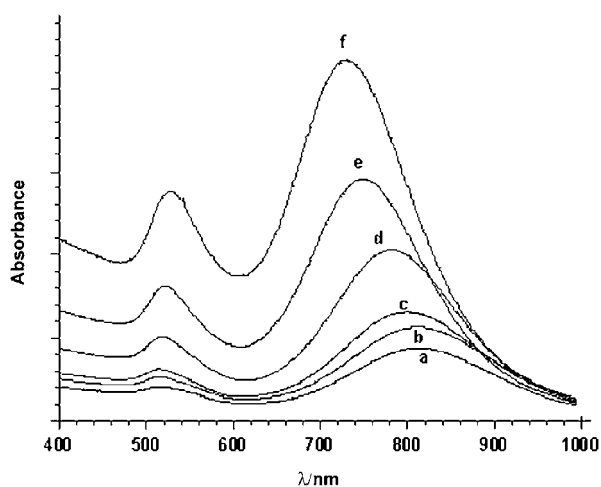


Figure 1. UV-visible spectra for the as-made Au nanorods (a) and after the Au overgrowth with addition of 7, 20, 60, 125, 250 μL (b–f, respectively) of a solution of HAuCl_4 .

dish-brown and displays two characteristic surface plasmon absorption peaks at 513 and 814 nm. Upon addition of HAuCl_4 and ascorbic acid, the absorption spectra changed depending on the HAuCl_4 concentration. The transverse plasmon absorption bands shift to the red slightly, while the longitudinal plasmon absorption bands shift to the blue significantly as the aspect ratio, the ratio of length to diameter,

of Au nanorods decreases; this is in good agreement with previous theoretical predictions.^[21] These UV-visible spectra clearly imply that as the concentration of HAuCl_4 increases, the overgrowth of the Au reduces the aspect ratio of the resulting Au nanorods gradually.

Figure 2 shows the TEM images of the as-made Au nanorods and the overgrown Au nanorod colloids as described in Figure 1. The side facets of the as-made nanorods are domi-

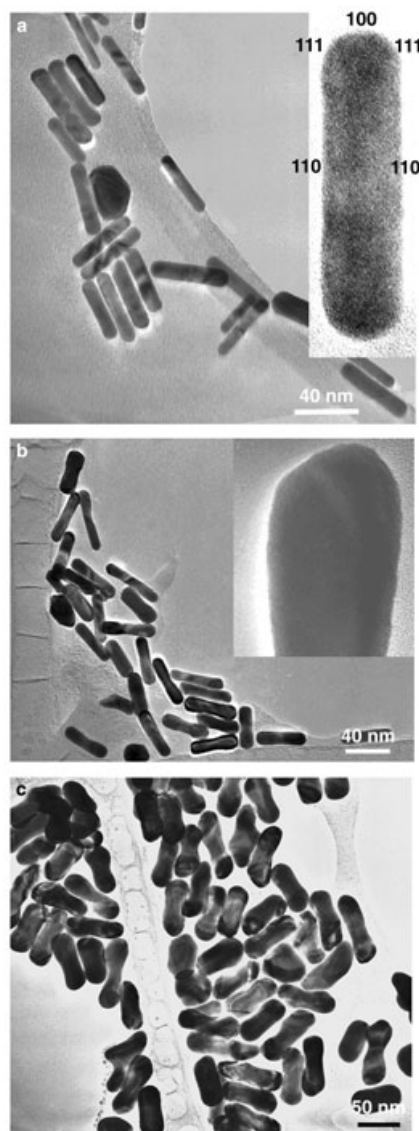


Figure 2. a) Transmission electron microscopy (TEM) image of the as-made Au nanorods. Inset shows a high resolution TEM image of a as-made nanorod displaying its {110} side surfaces and {111}, {100} end surfaces. b) TEM image of nanorods after initial overgrowth with addition of a solution of HAuCl_4 (7 μL). Inset shows a high resolution TEM image of a thin dumbbell-shaped nanorod. c) TEM image of nanorods after Au overgrowth with addition of a solution of HAuCl_4 (60 μL).

nated by the {110} planes with possible smaller {100} facets.^[22] Each nanorod has a faceted shape and is enclosed by at least four {110} facets. The ends of these nanorods are

enclosed by predominantly {111} and {100} planes, as indicated in Figure 2a inset. As the concentration of AuCl_4^- increases, dumbbell shapes of Au nanorods emerge prominently (Figure 2b,c). The shape evolution of a single nanorod during the overgrowth is shown in Figure 3. The arrows

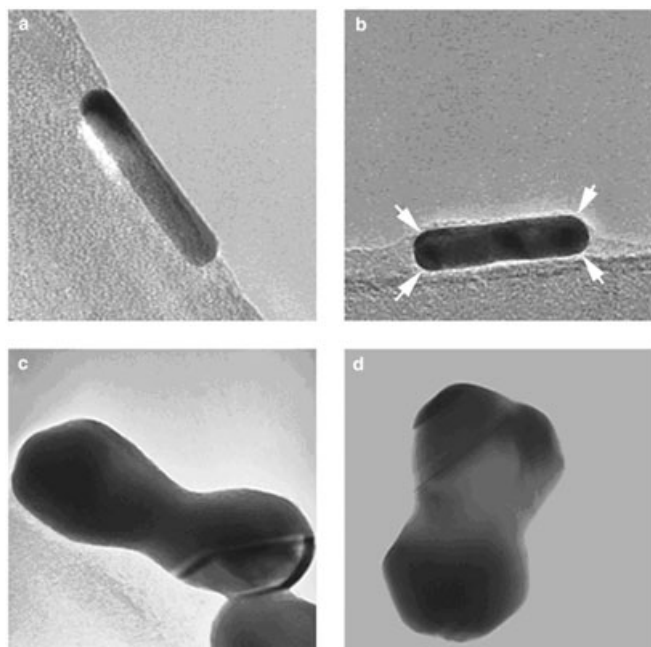


Figure 3. TEM images of a gold nanorod after Au overgrowth. a) as-made nanorod seed; b–d) after addition of 7, 125, 250 μL of a solution of HAuCl_4 , respectively. The arrows in (b) indicate the preferred growth sites.

in Figure 3b indicate the preferred Au overgrowth sites so that a dumbbell-shaped nanorod forms. These unusual dumbbell shapes suggest that the end {111} facet of Au nanorods is more amenable for overgrowth than the side {110} facets. A previous study revealed that these electrochemically prepared Au nanorods are stabilized by bilayers of the cationic surfactants. These surfactants are expected to bind much more strongly to the less-close packed {110} surface than to {111} or {100} facets.^[2b] Our results imply that these less stable {110} facets are less likely to be coated with Au due to stronger interaction with the surfactant molecules. Hence, the overgrowth rate along [111] directions would be higher than that along [110] directions. Overall, the two ends of nanorods get thicker and aspect ratio of the nanorods gets reduced.

Effect of silver-ion addition: We further examined the effect of silver-ion addition on the overgrowth of Au nanorods. The importance of silver ions in the preparation of gold nanorods has been previously observed in the electrochemical and photochemical synthesis of Au nanorods,^[5] whereby increasing silver-ion concentration resulted in increasing the aspect ratio of the Au rods. This effect has also recently been reported in seeded growth of Au nanoparticles/rods, in which the authors consider these silver ions as “shape-regu-

lating agents”.^[7] Hence, it would be fundamentally interesting to explore how the silver-ion addition could control the shape of the resulted nanorods in our process. After adding AgNO_3 to a solution mixture of cetyltrimethylammonium bromide (CTAB; 0.08 M, 5 mL), ascorbic acid (0.1 M, 0.25 mL), and Au nanorod colloids (0.1 mL), we did not observe the characteristic silver plasmon band at ~ 400 nm in UV-visible spectrum, from which we assume that the silver ions are not reduced by the weak reducing agent ascorbic acid; they most likely form AgBr in the solution and absorb onto the nanorod surface.

Figure 4 shows the UV-visible spectra of as made Au nanorods, Au overgrown Au nanorods, and Au overgrown Au nanorods in the presence of AgNO_3 . Upon addition of

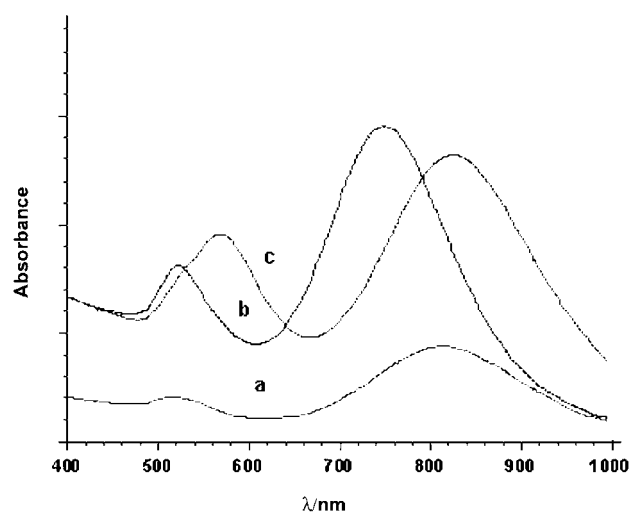


Figure 4. UV-visible spectra for the as-made Au nanorods (a) and after the Au overgrowth with addition of a solution of HAuCl_4 (125 μL) without Ag ion addition (b), and with addition of AgNO_3 (7 μL) (c).

Au nanorod colloids to an Au overgrowth solution (containing 5 mL of 0.08 M CTAB, 0.25 mL of 0.1 M ascorbic acid, and 0.125 mL of 0.01 M HAuCl_4), the surface plasmon absorption peaks shift; the 513 nm band red-shifts to 523 nm and the 814 nm band blue-shifts by ~ 67 nm due to shortened aspect ratio. When the seed was added to the Au growth solution (containing 5 mL of 0.08 M CTAB, 0.25 mL of 0.1 M ascorbic acid, and 0.125 mL of 0.01 M HAuCl_4) in the presence of AgNO_3 (13 μL , 0.01 M), it was found that the transverse surface plasmon absorption peak shifted to 568 nm with a shoulder near 513 nm, while longitudinal surface plasmon absorption peak remained almost unchanged.

TEM images of the nanorods after the overgrowth are shown in Figure 5. We observed a decreased tendency in the growth of Au shell in the presence of silver ions that may account for the unshifted longitudinal plasmon peak. The exact roles that silver ions play in regulating the shape of Au over-grown Au nanorods is not completely understood at this moment; however, based on our UV-visible and TEM studies, we propose that silver ions might adsorb on

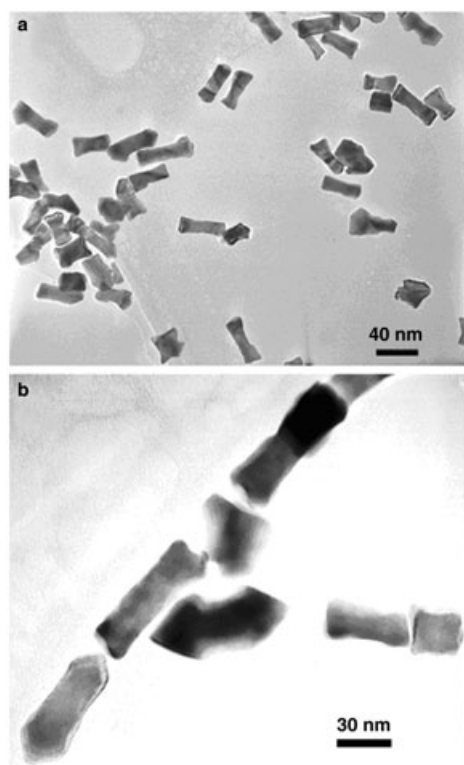


Figure 5. TEM images of gold nanorods after Au overgrowth with the AgNO_3 (a, 50 μL ; b, 75 μL) addition.

the surface of the Au nanorods and further retard the overgrowth of Au on the {110} side surfaces. In addition, as can be readily seen in Figure 5, the resulting nanorods became much more faceted, in fact, many of them turn into rectangular shape rather than the smooth dumbbell-shaped nanorods produced without silver-ion addition. This further indicates that the Ag ions play a subtle role in regulating growth rates on the {111}, {110}, and {100} planes; they may indeed be capable of promoting one-dimensional crystal growth. It is possible that the silver ions play similar roles in the previously reported silver-ion effect during the electrochemical Au nanorod growth as well as the seeded nanorod growth.^[5,7]

Effect of different reducing methods: In parallel with the chemical reduction method for Au overgrowth, we have also explored another reduction process. In this alternative approach, aqueous solutions of CTAB ($5 \times 10^{-4} \text{ M}$) and HAuCl_4 ($2 \times 10^{-3} \text{ M}$) were prepared. Small amounts of each solution (5 mL) were mixed together in a 20 mL vial. Aqueous NaOH solution (100 μL , 0.5 M) was added to adjust the pH to around 12. The solution became clear with the addition of NaOH and the gold nanorod solution (100 μL ; aspect ratio ~ 4.5) then was added. The resulting solution was irradiated with UV light (365 nm) for 2–3 h, upon which it turned blue. TEM studies (Figure 6) on the products indicate a high yield of Au nanowires with an average diameter of $\sim 6 \text{ nm}$. These Au nanowires are thin, continuous, and

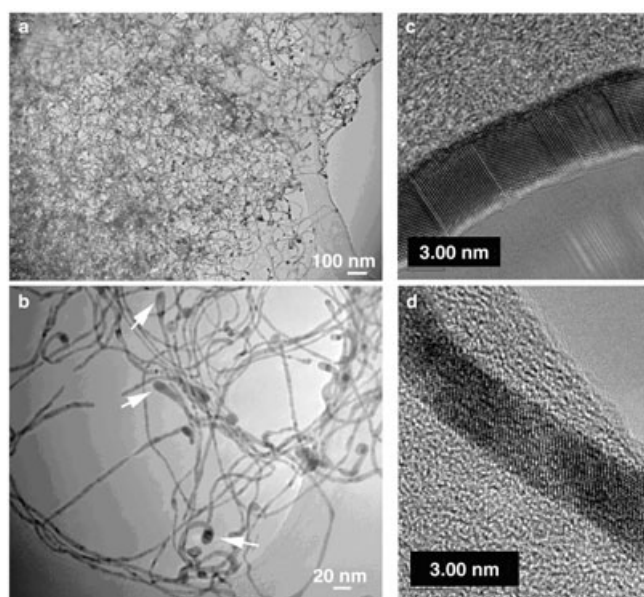


Figure 6. TEM images of thin gold nanowires produced with a photochemical reduction process using Au nanorods as seeds. The arrows in (b) indicate the possible nanorod seeds.

highly crystalline, as can be seen in Figure 6c–d. Control experiments without the addition of the gold nanorod seed solution were carried out; it was found that the nanowire yield decreased significantly. These results suggest that it is possible to use nanorods as seeds to significantly promote one-dimensional nanostructure growth in the presence of surfactants under photochemical conditions. Indeed, nanorod-shaped tips (indicated by arrows in Figure 6b) are frequently observed in these nanowires. The nanowires generated through this seeding process are generally much thinner than those reported by Esumi who used a similar surfactant system (but without seeding).^[14]

Au–Ag core–shell nanorods: Figure 7 shows the UV-visible absorption spectra of nanorod colloids prepared by the reduction of AgNO_3 with ascorbic acid in the presence of Au nanorod seed, together with the spectrum of initial Au nanorods. The addition of NaOH is necessary to enhance the reducing capability of the ascorbic acid.^[7] Upon the Ag overgrowth, a visible color change occurred from yellow to brown, depending on Au nanorod seed concentration. Both transverse and longitudinal surface plasmon absorption bands shift to the blue with silver coating. The transverse plasmon band gradually red shifts (387 to 410 nm) as the Au nanorod colloid concentration is decreased from 0.2 (Figure 7c) to 0.1 mL (Figure 7b), suggesting the formation of thickly coated $\text{Au}_{\text{core}}\text{Ag}_{\text{shell}}$ nanorods. The thickly coated nanorods show the longitudinal plasmon band at a much shorter wavelength (618 nm, Figure 7b) than the thinly coated nanorods (744 nm, Figure 7c). It was clearly seen that when the silver-layer thickness is increased as the seed concentration is decreased, the transverse plasmon band of the composite nanorods shifts to the red and the optical

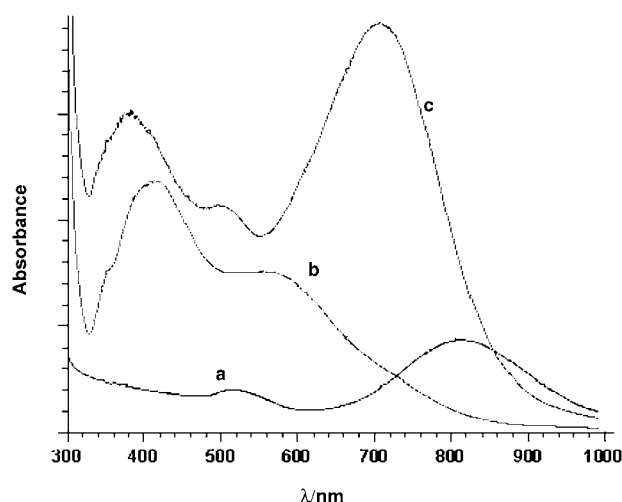


Figure 7. UV-visible spectra for the as-made Au nanorods (a) and after the Ag overgrowth with addition of 0.1 mL (b) and 0.2 mL (c) Au nanorod stock solution.

properties of $\text{Au}_{\text{core}}\text{Ag}_{\text{shell}}$ nanorods are dominated by the silver shell.^[23] This observation is also in agreement with the previously reported nanorod overgrowth through NH_2OH reduction of AgCl_4^{3-} .^[19]

Figure 8 shows the TEM images of $\text{Au}_{\text{core}}\text{Ag}_{\text{shell}}$ nanorods prepared with 0.1 mL of Au nanorod solution. It is evident from the TEM images that these core-shell nanorods have good monodispersity. Note Au and Ag have similar lattice parameters of 0.4078 nm and 0.4086 nm, respectively. This allows epitaxial crystal growth of Ag on Au nanorod surfaces. Figure 8b shows a high resolution TEM image of a clean Ag/Au interface. In addition, elemental analysis was also carried out across the interface by means of energy dispersive X-ray spectroscopy. Figure 8c shows a line profile of the Ag and Au composition that traverses the Ag–Au core-shell nanorod axis; this further demonstrates a sharp interface between Ag and Au.

Au–Pd core-shell nanorods: Considerable efforts have been made on the control of the size of palladium nanoparticles, as it is well known that the catalytic reactivity and selectivity are strongly dependent on their size. Palladium is an important hydrogenation catalyst and it was found that that $\text{Au}_{\text{core}}\text{Pd}_{\text{shell}}$ nanoparticles are more efficient than Pd itself.^[24] The growth of a Pd shell on the Au nanorod surface could be readily followed by UV-visible spectrophotometry. Figure 9 shows the UV-visible spectra of the as-made Au nanorods and the $\text{Au}_{\text{core}}\text{Pd}_{\text{shell}}$ nanorod colloids. The color of the Au nanorod colloids changed to brown, suggesting the formation of palladium nanoparticles. Figure 9b shows a brownish absorption without any observable peaks. The $\text{Au}_{\text{core}}\text{Pd}_{\text{shell}}$ bimetallic nanoparticles have been shown to exhibit no characteristic absorption from Au clusters as the Pd shell thickness increases.^[25]

Figure 10 shows TEM images of $\text{Au}_{\text{core}}\text{Pd}_{\text{shell}}$ nanorods. We observed uniform heterogeneous $\text{Au}_{\text{core}}\text{Pd}_{\text{shell}}$ nanorods,

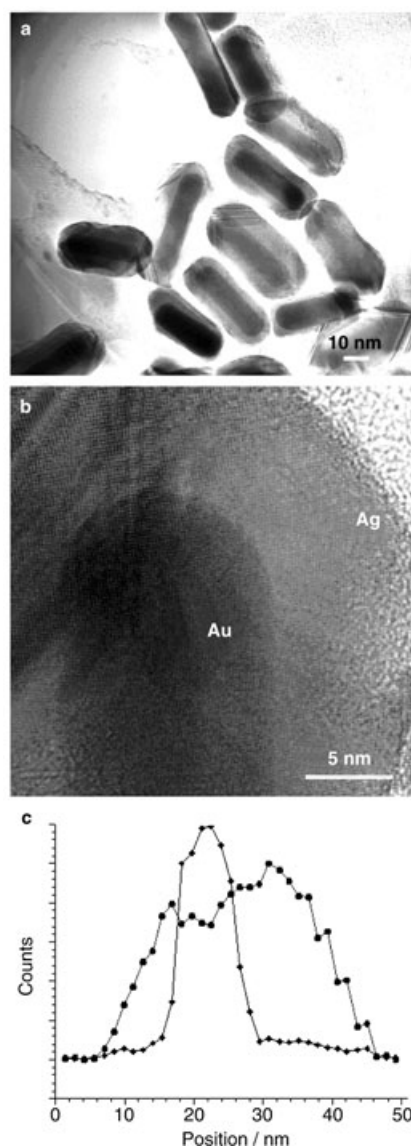


Figure 8. a) and b) TEM images of gold nanorods after Ag overgrowth. c) Line profile of Au (—◆—) and Ag (—●—) concentration transversing the nanorod axis probed by energy dispersive X-ray spectroscopy.

which are built up by a gold core surrounded by palladium nanocrystals of about 2–4 nm diameter. As the concentration of H_2PdCl_4 increases, individual Pd nanocrystals start fusing together. The energy dispersive X-ray (EDX) microanalysis shows that the prepared core-shell nanorods material consists of gold and palladium only. The compositional line profile (Figure 10b) of the transversal cross-section of $\text{Au}_{\text{core}}\text{Pd}_{\text{shell}}$ nanorod demonstrates that palladium shell is uniform throughout the surface of Au nanorod.

Conclusion

The overgrowth on the nanorod surface is a quite complex process that is directly related to nanorod formation mecha-

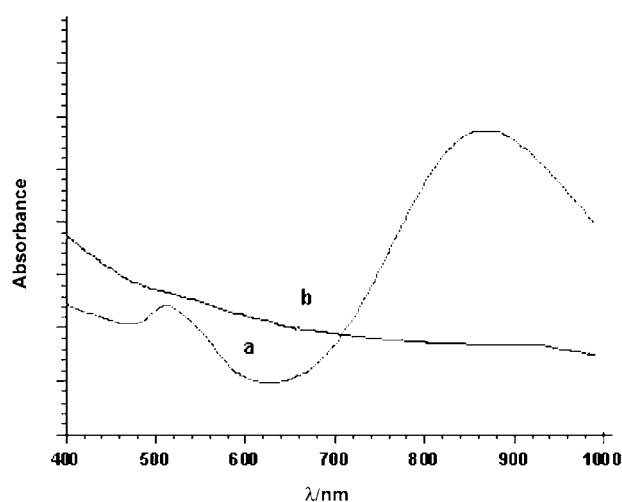


Figure 9. UV-visible spectra for a) the as-made Au nanorods and b) after Pd overgrowth.

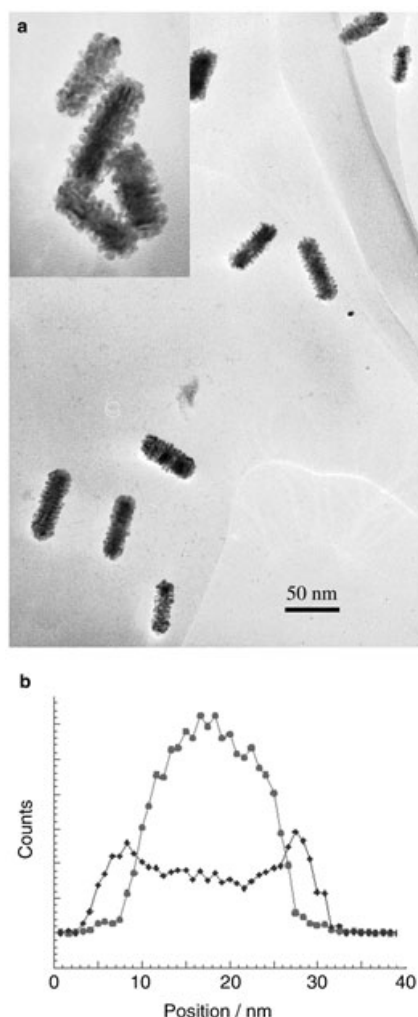


Figure 10. a) TEM images of gold nanorods after Pd overgrowth. Inset shows a high magnification view of the Au-Pd core-shell nanorods. b) Line profile of Au (●) and Pd (◆) concentration transversing the nanorod axis probed by energy dispersive X-ray spectroscopy.

nism. Among the three systems explored in this study, we note that the Ag and Au overgrowth essentially yields single-crystalline thin-shell coating, while the Pd overgrowth is polycrystalline. We believe this is a direct result of lattice mismatch between the Au nanorod and the overgrowth materials. The lattice constant of Pd (3.89 Å) is smaller than those of Ag and Au (4.08 Å). This lattice mismatch may induce the island nucleation/growth of Pd nanoclusters on Au nanorod surfaces. However, this polycrystalline nature of the Pd overgrowth may be beneficial for its potential catalytic applications due to its high surface area.

Unlike spherical particles in which the {111} surface generally dominates, the electrochemically synthesized nanorods exhibit predominantly {110} side surfaces as well as small percentage of {111} and {001} end surfaces. The competition of the overgrowth on these different surface facets results in highly anisotropic overgrowth pattern. In general, it was found that the {110} facets are less accessible for the overgrowth, due to possible stronger interactions with the cationic surfactants, relative to the {111} and {100} surfaces. This anisotropic overgrowth rate leads into the formation of dumbbell shapes nanorods in the Ag and Au overgrowth systems. The overgrowth rates can be further adjusted by adding foreign ions and by using different reducing chemistry, as exemplified here by the Ag effect and the photochemical nanowire formation using nanorods as seeds.

Electrochemically prepared Au nanorods were used as seeds for the overgrowth of thin shells of gold, silver, and palladium by using a mild reducing agent, ascorbic acid, in the presence of surfactants at ambient condition. The use of weak reducing agent is important in order to achieve well-defined shell growth, while avoiding effectively undesired homogeneous nucleation. Since the starting nanorods exhibit unique crystal facets, the overgrowth exhibits interesting features due to competing growth on different side facets. This overgrowth behavior should provide insights on how different metal ions could be reduced preferentially on Au nanorod surfaces so that the composition, aspect ratio, shape, and facet of the resulting nanostructures can be rationally tuned. These surfactant-stabilized bimetallic Au_{core}-M_{shell} (M = Au, Ag, Pd) nanorod colloids could serve as better substrates for surface-enhanced Raman spectroscopy, chemical/biological sensing, and catalysis.

Experimental Section

Gold nanorod synthesis: Gold nanorods were synthesized by using an electrochemical reaction.^[5a] An aqueous solution of hexadecyltrimethylammonium bromide (CTAB, 0.08 M) and tetradodecylammonium bromide (4.2 mg/ml) was used as the electrolyte. Gold and platinum metal plates were used as the anode and cathode. The electrolyte solution (4 mL), cyclohexane (48 μL), and acetone (88 μL) were used in each reaction. A constant current of 5 mA was applied to the system for 27 minutes. In order to produce rods, a silver plate was immersed in the electrolyte before the reaction. The solution was collected after the reaction, and centrifuged at 12000 rpm for 20 minutes. The flocculates were collected, redispersed in DI (4 mL) and used as stock solution.

Overgrowth of Au on Au nanorods: In a clean vial, HAuCl₄ (0.007–0.125 mL, 0.01 M) was added into a solution containing CTAB (5 mL, 80 mM), electrochemically synthesized Au nanorod^[5] colloid as seeds (0.1 mL), and freshly prepared ascorbic acid solution (0.012–0.25 mL, 0.1 M). The solution was sonicated at room temperature during preparation. Absorption spectra of the nanorod dispersions were taken using a HP8453 UV-visible spectrophotometer. The resulting Au nanorods were separated from excess surfactants by centrifugation at 2000 rpm for 10 min. The supernatant was removed and the precipitate was redispersed in deionized water (0.5 mL), which was used later for transmission electron microscopy (TEM) analysis.

Synthesis of Au_{core}Ag_{shell} nanorods: To make Au_{core}Ag_{shell} nanorods, AgNO₃ was reduced by ascorbic acid in the presence of Au nanorods, the micellar template CTAB, and NaOH. Two sets of solution containing CTAB (5 mL, 80 mM), AgNO₃ (0.125 mL, 10 mM), and ascorbic acid (0.25 mL, 0.1 M) were prepared. Next, different amount of Au nanorods (0.1 and 0.2 mL) were added, respectively, and then NaOH (0.05 mL, 0.5 M) was added slowly while stirring. UV-visible absorption spectra were taken using a HP 8453 spectrophotometer. The Au_{core}Ag_{shell} nanostructures were separated from excess surfactant by centrifugation at 2000 rpm for 15 min. The supernatant was removed and the precipitate was redispersed in deionized water (0.5 mL), which was used later for TEM and energy dispersive X-ray (EDX) elemental analysis.

Synthesis of Au_{core}Pd_{shell} nanorod colloid: H₂PdCl₄ was prepared from PdCl₂ (0.0355 g), dissolved in HCl (2 mL, 0.2 M), and diluted to 100 mL with de-ionized water. Electrochemically prepared Au nanorod colloids (0.1 mL) were added into the mixture of CTAB (5 mL, 0.08 M), H₂PdCl₄ (0.125 mL, 2 mM), and freshly prepared ascorbic acid (0.25 mL, 0.1 M). All the solutions were under sonication during the preparation. UV-visible absorption spectra were measured using a HP 8453 spectrophotometer. Au_{core}Pd_{shell} nanorods were separated from excess surfactant by centrifugation at 2000 rpm for 10 min. The supernatant was removed and the precipitate was re-dispersed in de-ionized water (0.5 mL), which was used later for TEM and EDX microanalysis.

Acknowledgement

P.Y. is an Alfred P. Sloan Research Fellow. Work at the Lawrence Berkeley National Laboratory was supported by the Office of Science, Basic Energy Sciences, Division of Materials Science of the U.S. Department of Energy. We thank the National Center for Electron Microscopy for the use of their facilities and A. Fu for carrying out some of the wire experiments.

[1] J. A. Creighton, D. G. Eadon, *J. Chem. Soc. Faraday Trans.* **1991**, 87, 3881.

- [2] a) S. Link, M. A. El-Sayed, *J. Phys. Chem. B* **1999**, 103, 8410; b) B. Nikoobakht, M. A. El-Sayed, *Langmuir* **2001**, 17, 6368; c) Z. L. Wang, *J. Phys. Chem. B* **2000**, 104, 1153.
- [3] Y. W. Cao, R. Jin, C. A. Mirkin, *J. Am. Chem. Soc.* **2001**, 123, 7961.
- [4] a) X. Peng, L. Manna, W. Yang, J. Wickham, E. Scher, A. Kadavani, A. P. Alivisatos, *Nature* **2000**, 404, 59; b) V. F. Puntes, K. M. Krishnan, A. P. Alivisatos, *Science* **2001**, 291, 2115.
- [5] a) S. Chang, C. Shih, C. Chen, W. Lai, C. R. C. Wang, *Langmuir* **1999**, 15, 701; b) F. Kim, J. H. Song, P. Yang, *J. Am. Chem. Soc.* **2002**, 124, 14316.
- [6] M. Li, H. Schnablegger, S. Mann, *Nature* **1999**, 402, 393.
- [7] a) N. R. Jana, L. Gearheart, C. J. Murphy, *Chem. Commun.* **2001**, 617; b) N. R. Jana, L. Gearheart, C. J. Murphy, *Adv. Mater.* **2001**, 13, 1389.
- [8] S. J. Park, S. Kim, S. Lee, Z. G. Khim, K. Char, T. Hyeon, *J. Am. Chem. Soc.* **2000**, 122, 8581.
- [9] B. Nikoobakht, Z. L. Wang, M. A. El-Sayed, *J. Phys. Chem. B* **2000**, 104, 8635.
- [10] H. Maeda, Y. Maeda, *Langmuir* **1996**, 12, 1446.
- [11] Y. G. Sun, B. Gates, B. Mayers, Y. N. Xia, *NanoLett* **2002**, 2, 165.
- [12] a) F. Kim, S. Kwan, J. Akana, P. Yang, *J. Am. Chem. Soc.* **2001**, 123, 4360–4361; b) F. Kim, J. Arkana, P. Yang, *Chem. Commun.* **2001**, 5, 447.
- [13] B. R. Martin, D. J. Dermody, B. D. Reiss, M. M. Fang, L. A. Lyon, M. J. Natan, T. E. Mallouk, *Adv. Mater.* **1999**, 11, 1021.
- [14] K. Esumi, K. Matsuhisa, K. Torigoe, *Langmuir* **1995**, 11, 3285.
- [15] Y. Mizukoshi, T. Fujimoto, Y. Nagata, R. Oshima, Y. Maeda, *J. Phys. Chem. B* **2000**, 104, 6028.
- [16] A. Henglein, *J. Phys. Chem. B* **2000**, 104, 2201.
- [17] J. H. Hodak, A. Henglein, G. V. Hartland, *J. Phys. Chem. B* **2000**, 104, 5033.
- [18] M. Hosteler, C.-J. Zhong, B. K. H. Yen, J. Anderegg, S. M. Gross, N. D. Evans, M. Porter, R. W. Murray, *J. Am. Chem. Soc.* **1998**, 120, 9396.
- [19] a) C. S. Ah, S. D. Hong, D. J. Jang, *J. Phys. Chem. B* **2001**, 105, 7871; b) M. Liu, P. Guyot-Sionnest, *J. Phys. Chem. B* **2004**, 108, 5882; c) C. Huang, Z. Yang, H. Chang, *Langmuir*, **2004**, 20, 6089.
- [20] L. Lu, H. Wang, Y. Zhou, S. Xi, H. Zhang, J. Hu, B. Zhao, *Chem. Commun.* **2002**, 144.
- [21] S. Link, M. A. El-Sayed, *J. Phys. Chem. B* **1999**, 103, 8410.
- [22] Z. L. Wang, M. B. Mohamed, S. Link, M. A. El-Sayed, *Surf. Sci.* **1999**, 440, L809.
- [23] C. F. Bohren, D. F. Huffmann, *Absorption and Scattering of Light of Small Particles*, Wiley, New York, **1983**, p. 183.
- [24] G. Schmid, H. West, J. Malm, J. Bovin, C. Grenthe, *Chem. Eur. J.* **1996**, 2, 1099.
- [25] N. Toshima, H. Harada, Y. Yamazaki, K. Asakura, *J. Phys. Chem.* **1992**, 96, 9927.

Received: August 5, 2004
Published online: December 9, 2004